American Mineralogist, Volume 83, pages 1335–1339, 1998

Rubicline, a new feldspar from San Piero in Campo, Elba, Italy

David K. Teertstra,[1] Petr Černý,[1] Frank C. Hawthorne,[1,*] Julie Pier,[2] Lu-Min Wang,[2,†] and Rodney C. Ewing[2,†]

[1]Department of Geological Sciences, University of Manitoba, Winnipeg, Manitoba, Canada R3T 2N2
[2]Department of Earth and Planetary Sciences, University of New Mexico, Albuquerque, New Mexico 87131-1116, U.S.A.

Abstract

The rubidium analogue of microcline, rubicline, $(Rb,K)AlSi_3O_8$, ideally $RbAlSi_3O_8$, was found in a pollucite-bearing rare-element pegmatite at San Piero in Campo, Elba, Italy. Rubicline is the first mineral with rubidium as an essential constituent. It occurs as abundant but small (≤50 μm) rounded grains in 1–2 cm wide veins of rubidian microcline (± albite, muscovite, quartz, and apatite) that crosscut pollucite. Rubicline is brittle, transparent, and colorless. Refractive indices are slightly higher than those of the host microcline. The birefringence is low (1st order gray interference colors), and crystals are apparently untwinned. In thin and polished sections, cleavage passes through both the host microcline and grains of rubicline; by analogy with microcline, the cleavage is {001} perfect and {010} good. Determination of additional physical properties is hindered by an average grain size of 20 μm, heterogeneous composition, and structural coherency of rubicline with the enveloping microcline. Rubicline is triclinic, probable space group $P\bar{1}$, with a = 8.81(3), b = 13.01(3) c = 7.18(4) Å, α = 90.3(1), β = 115.7(3), γ = 88.2(1)°, V = 741 Å^3, Z = 4, and axial ratios $a:b:c$ of 0.677:1:0.577 (calculated from electron-diffraction data). Chemical analysis by electron microprobe gave 58.68 SiO_2, 16.48 Al_2O_3, 6.23 K_2O, 17.47 Rb_2O, 0.92 Cs_2O, 0.12 Fe_2O_3, sum 99.90 wt% and the formula $(Rb_{0.574}K_{0.407}Cs_{0.020})_{\Sigma 1.001}(Al_{0.993}Fe_{0.005})Si_{3.001}O_8$. Rubicline is, in many cases, structurally coherent with the host microcline; it formed by exsolution from a (K,Na,Rb)-enriched precursor, followed possibly by fluid-induced modification.

Introduction

The granitic pegmatites of Elba, Italy, contain various rare-element minerals and are a source of valuable gemstock (Orlandi and Scortecci 1985). Pollucite and petalite were first described from Elba (Breithaupt 1846). Foitite was recently discovered in the Filone-Rosina aplite-pegmatite dyke, which has produced many fine specimens of tourmaline (Pezzotta et al. 1996). During systematic study of the minerals that form part of the typical sequence of alteration of pollucite, several occurrences of Rb-dominant feldspars were found (Teertstra et al. 1998a). These represent the first mineral(s) in which rubidium is an essential constituent.

Rubidium-dominant feldspar is relatively widespread in the core zones of complex (Li,Cs,Rb)-enriched rare-element granitic pegmatites that contain Rb-rich potassium feldspars associated with pollucite. However, in the dozen-or-so pegmatites in which feldspars with Rb > K were identified, small grain size, optical similarity to microcline, and structural coherency with host microcline precluded manual separation of rubicline for the purpose of structural characterization. The small size, the similarity of rubicline to microcline in thin section, and the similar X-ray powder-diffraction patterns probably hindered earlier identification. By electron microprobe, the energy dispersive (EDS) Rb$L\alpha$ peak is hidden under the Si$K\alpha$ peak, leaving only wavelength dispersive (WDS) analysis and backscattered electron (BSE) imaging as methods of detecting rubicline. However, the rubicline structure was shown to be similar to that of triclinic (Al,Si)-ordered microcline using high-resolution transmission electron microscopy (HRTEM) on the Elba material. The new mineral and name have been approved by the Commission on New Minerals and Mineral Names, IMA. The original sample was a single unregistered fragment from the Ecole des Mines, Paris collection. Two halves of the type material are deposited in the R.B. Ferguson Museum of Mineralogy, University of Manitoba under catalogue numbers M 6980 and M 6981.

Occurrence

The Monte Capanne monzogranitic pluton is well exposed at the western end of the island of Elba, Tyrrhenian Sea, Italy. Numerous rare-element pegmatites occur along the eastern margin of the pluton, but pollucite is known only from the pegmatite veins near San Piero in Campo;

* E-mail: frank_hawthorne@umanitoba.ca
† Present address: Department of Nuclear Engineering and Radiological Sciences, University of Michigan, Ann Arbor, MI 48109-2104, U.S.A.

0003–004X/98/1112–1335$05.00

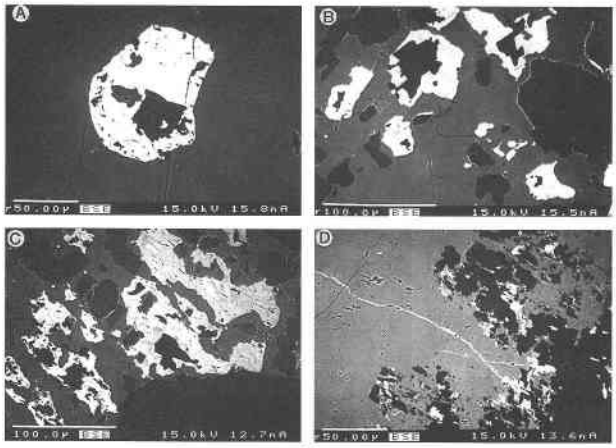

FIGURE 1. BSE images of rubicline from Elba: (**A**) Large grain of rubicline (white) + quartz (black) in microcline (dark gray); (**B**) Rubicline (white) including grains of quartz (black) in microcline (gray) associated with albite (black) and muscovite (mottled dark gray); (**C**) Rubicline (white) + quartz (black) in microcline (gray) in contact with Rb-free adularia (dark gray) at margins; (**D**) Veinlet of rubicline (white) in microcline (gray) and small grains of rubicline (white) associated with albite (black).

these include La Speranza, Fonte del Prete, Filone della Speranza, and Masso Foresi (Orlandi and Scortecci 1985). The sample investigated here (Ecole des Mines, Paris) is probably from the La Speranza dyke. In the Elba granitic pegmatites, pollucite occurs at the margins of miarolitic cavities, in association with primary microcline, albite, muscovite, quartz, and elbaite; it is strongly corroded and locally overgrown by late-stage zeolites. Our sample of pollucite follows the typical sequence of alteration of pollucite from other localities (Teertstra et al. 1993): coarse (1–2 cm wide) veining by coarse-grained lepidolite and microcline (± muscovite), fine (1–2 mm wide) veining by fine-grained muscovite (± spodumene), local metasomatic replacement by untwinned non-perthitic near-Or_{100} adularia, followed by late analcimization, leaching, and argillization.

Numerous small (<20–50 μm) grains of rubicline (+ quartz) occur in 1–2 cm wide veins of twinned microcline (+ muscovite with 1.4–1.7 wt% Rb_2O, albite Ab_{100}, and minor apatite with 4.1 wt% MnO) which crosscut pollucite (Figs. 1A–1C). The host microcline has patchy distributions of 0.11–0.35 wt% Na_2O, 0.90–3.39 wt% Rb_2O, and 0.10–0.31 wt% Cs_2O; most microcline is P-free, but local concentrations reach 0.35 wt% P_2O_5. Average Rb_2O content of the microcline corresponds to approximately 5 mol% Rbf (rubidium feldspar). Rubicline also occurs with albite, and locally forms thin (<5 μm wide) veinlets in microcline (Fig. 1D). Minor quantities of (Rb,K)-rich feldspar occur with metasomatic untwinned adularia (+ cookeite) that overgrows microcline and replaces microcline and pollucite along grain boundaries (Fig. 1C). The adularia is Na-, P-, and Rb-free with BaO ≤ 0.16 wt% and SrO ≤ 0.16 wt%. The adularian (Rb,K)-rich feldspar is Na- and P-free with 8.45–18.86 wt% Rb_2O and 0.17–1.69 wt% Cs_2O (Table 1).

PHYSICAL AND OPTICAL PROPERTIES

Rubicline is brittle, transparent, and colorless. Refractive indices are slightly higher than those of the host microcline as determined by Becke-line tests in thin section.

TABLE 1. Representative compositions of K-Rb feldspars from San Piero in Campo, Elba, Italy

Oxide	1	2	3	4	5	6	7	8
SiO_2	63.34	64.00	58.68	60.77	58.42	56.96	64.80	57.89
Al_2O_3	18.25	18.12	16.48	17.27	15.84	16.32	18.24	16.65
P_2O_5	0.25	0.00	0.00	0.00	0.00	0.00	0.01	0.00
Na_2O	0.30	0.14	0.00	0.02	0.00	0.00	0.00	0.00
K_2O	15.60	15.51	6.23	10.35	4.16	3.75	16.56	5.08
Rb_2O	0.90	1.66	17.47	10.90	19.61	21.55	0.00	18.86
Cs_2O	0.25	0.22	0.92	0.38	1.37	1.10	0.02	0.78
SrO	0.00	0.00	0.00	0.03	0.09	0.08	0.02	0.07
BaO	0.00	0.09	0.00	0.00	0.00	0.00	0.00	0.00
Sum	98.89	99.74	99.90	99.72	99.49	99.76	99.65	99.33
Si	2.980	2.999	3.001	2.996	3.032	2.990	3.006	2.991
Al	1.012	1.001	0.991	1.003	0.969	1.010	0.997	1.014
P	0.010	0.000	0.000	0.000	0.000	0.000	0.000	0.000
Na	0.027	0.013	0.000	0.002	0.000	0.000	0.000	0.000
K	0.936	0.927	0.407	0.651	0.276	0.251	0.980	0.335
Rb	0.027	0.050	0.574	0.345	0.654	0.727	0.000	0.626
Cs	0.005	0.004	0.020	0.008	0.030	0.025	0.000	0.017
Sr	0.000	0.000	0.000	0.001	0.003	0.002	0.000	0.002
Ba	0.000	0.002	0.000	0.000	0.000	0.000	0.000	0.000
ΣM	0.995	0.996	1.000	1.007	0.963	1.005	0.980	0.980
M^+	0.995	0.998	1.000	1.008	0.966	1.007	0.980	0.982
TO_2^-	1.002	1.001	0.998	1.003	0.969	1.010	0.997	1.014
ΣT	4.002	4.001	3.999	3.999	4.001	4.000	4.004	4.008
Si/Al	2.99	3.00	3.00	2.99	3.13	2.96	3.02	2.94

Note: Atomic contents based on 8 atoms of oxygen. 1 and 2 = Microcline veins in pollucite. 3 = Representative composition of rubicline characterized structurally by HRTEM; includes 0.12 Fe_2O_3 (0.005 apfu). 4 = Rubidian microcline associated with albite in microcline vein. 5 and 6 = Rubicline in microcline. 7 = Adularia replacing pollucite. 8 = Rb-K feldspar in adularia.

Rubicline is biaxial, but it was not possible to measure 2V. Grains positively identified in thin section show low birefringence (1st order gray interference colors) and an apparent lack of twinning. In thin and polished sections, cleavage passes through both the host microcline and grains of rubicline (Fig. 1A); by analogy with microcline, the cleavage is {001} perfect and {010} good. Determination of additional physical properties is hindered by an average grain size of 20 μm, compositional variability and structural coherency of exsolved rubicline and host microcline.

Chemical composition

The Rb-K feldspars were analyzed using WDS analysis on a CAMECA SX-50 electron microprobe operating at 15 kV and 20 nA with a beam diameter of 5 μm. Data were reduced using the PAP procedure of Pouchou and Pichoir (1985). Major elements were measured using sanidine from Eifel, Germany (K$K\alpha$, Al$K\alpha$, and Si$K\alpha$) and synthetic $Rb_2ZnSi_5O_{12}$ glass (Rb$L\alpha$). The composition of the sanidine had been optimized to agreement with ideal feldspar stoichiometry according to the procedure of Teertstra et al. (1998b). The accuracy of the results is within 2%, and the precision is approximately 1% (4σ). Minor elements were measured using albite (Na$K\alpha$), pollucite (Cs$L\alpha$), fayalite (Fe$K\alpha$), barite (Ba$L\beta$), $SrTiO_3$ (Sr$L\alpha$), and VP_2O_7 (P$K\alpha$). The elements Ca, Mg, F, Pb, Mn, Ga, and Ti were sought but not detected.

Feldspar formulae were calculated on the basis of eight atoms of oxygen per formula unit (apfu). To compare compositions of P-free feldspar with feldspar locally containing P, the framework charge was calculated using TO_2^- = (Al + Fe^{3+}-P) and Si was adjusted using Si + 2P according to the (AlP)Si_{-2} berlinite substitution. Minor concentrations of P are found in the microcline, but P is absent from rubicline, adularia, and associated adularian Rb,K-rich feldspar (Table 1).

In the BSE images of Figure 1, gray levels of K-Rb feldspar increase with mole percent rubidium feldspar. Individual grains of microcline-hosted rubicline display a slight compositional heterogeneity (Figs. 1A and 1C). Clusters of grains have a slightly greater compositional range than individual grains. Overall, Rb_2O concentrations exsolved blebs of Rb-enriched to Rb-dominant feldspar throughout microcline range from ~10 to ~22 wt%, corresponding to ~30 to ~70 mol% Rbf.

Individual values for M-cation charge [M^+ = monovalent cations + 2×(divalent cations)] tend to be slightly lower than calculated values of framework charge (TO_2^- = Al + Fe-P), suggesting that minor (<1 at%) concentrations of light-element M-cations may be present locally (Fig. 2A). Values of (Si + 2P) cluster near 3.0 apfu for microcline, adularia, and adularian K-Rb feldspar; for rubicline, the data lie along the trend for the $\square Si_4O_8$ substitution (Fig. 2B). High Si/Al ratios correspond to low M-cation sums and equally low (Al-P); an extreme value with ~3% $\square Si_4O_8$ has Si = 3.032 (or 3.000 + 0.032) apfu, Al = 0.969 apfu, M^+ = 0.966 (or 1–0.034) pfu,

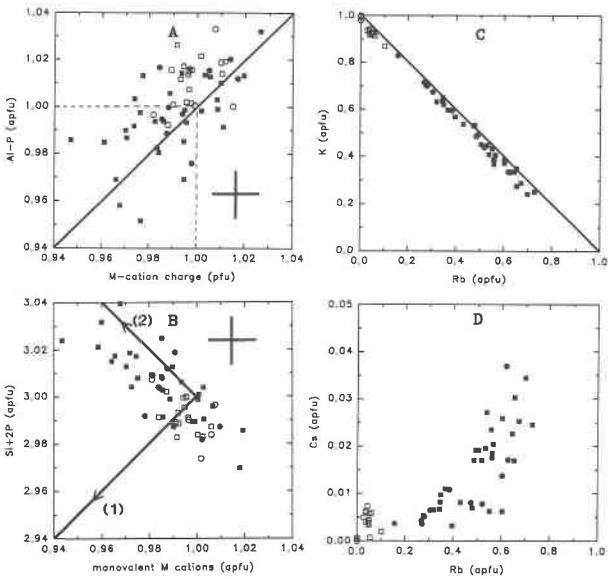

Figure 2. Element variations in K-Rb feldspars from Elba: (**A**) (Al+Fe-P) vs. M-cation charge with a 1:1 trend line; (**B**) (Si+2P) vs. the sum of monovalent M cations; (**C**) K vs. Rb, with a line indicating ΣM = 1; (**D**) Cs vs. Rb. Symbols: microcline vein in pollucite (□) and associated rubicline (■); late adularia (○) and associated (Rb,K)-feldspar (●).The arrows mark trends for (1) the plagioclase-like substitutions and (2) the $\square Si_4O_8$ substitution.

and ΣT = 4.001 apfu (no. 5 in Table 1). Extreme values for Rb_2O in the rubicline correspond to 72.7 mol% $RbAlSi_3O_8$ (Fig. 2C). In the Rb-richest samples, maximum substitution of Cs is 0.04 apfu, i.e., 4 mol% of a hypothetical cesium feldspar component (Fig. 2D).

TEM analysis of the structure

Attempts to separate rubicline yielded a microcline + feldspar with Rb > K + quartz mixture. X-ray powder diffraction of this mixture did not show the presence of phases other than feldspar and quartz, thereby establishing the absence of any potential non-feldspathic structure that could be attributed to a (Rb,K)$AlSi_3O_8$ compound. As the cell parameters of the vein microcline [a = 8.597(7), b = 12.963(6), c = 7.210(5) Å, α = 90.62(13), β = 115.99(2), γ = 87.87(13)°, V = 721.8(7) Å^3] are close to those of ideal maximum microcline, an exsolved feldspar phase coherent with this structure can also be expected to have a high degree of (Al,Si) order.

After identification of areas relatively abundant in rubicline by BSE imaging, several 3 mm diameter disks were drilled from the thin section for TEM examination. Petropoxy between the sample and glass was removed by ~24 h oxidation in a Technics Plasma Excitor using oxygen gas. Slotted copper disks were then glued to the sample using Superglue. Samples were thinned to electron transparency using a Gatan Duo-Mill ion mill with argon gas. Identification of Rb-rich areas relative to the milled hole was possible only by multiple cycles of mill-

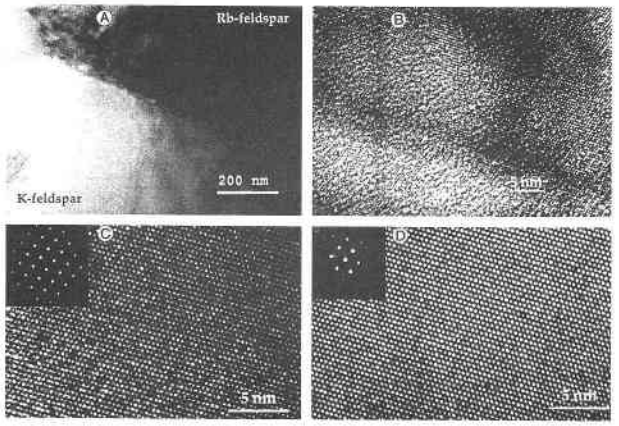

FIGURE 3. TEM micrographs: (**A** and **B**) the interface between rubicline and microcline; (**C** and **D**) high-resolution "lattice" image and SAED pattern of rubicline and microcline, respectively.

ing and location using BSE imaging on a scanning electron microscope (SEM). Once rubicline had been intersected by margins of the ion-milled area, samples were carbon-coated and examined on a JEOL 2000FX scanning transmission electron microscope equipped with a Noran 5500 EDS system and a JEOL 2010 HRTEM equipped with a Link ISIS EDS system.

The peaks for Si$K\alpha$ (at 1.740 keV) and Rb$L\alpha$ (at 1.694 keV) overlap in EDS analysis, and the Rb$K\alpha$ peak (at 13.375 keV) was used for analysis of Rb and identification of Rb-rich areas. Natural compositionally homogeneous triclinic rubidian microcline from Kola Peninsula, Russia [of composition $\sim(K_{0.70}Rb_{0.30})AlSi_3O_8$; Teertstra et al. 1997] was used as a standard for quantitative analysis. The alkali content of the structurally characterized rubicline from Elba, measured using EDS analysis, is approximately $Rb_{0.69}K_{0.31}$ apfu.

A bright-field image (Fig. 3A) shows a fairly sharp interface between rubicline and microcline. High-resolution images of the interface between rubicline and microcline indicate continuity of the structure (Fig. 3B), and individual diffraction patterns of rubicline and adjacent microcline show that both have the same crystallographic orientation (Figs. 3C and 3D). However, there is an increase in *d*-spacings from the Rb-poor microcline to the Rb > K areas of rubicline (Table 2). Diffraction patterns were indexed using cell parameters of synthetic triclinic rubidium feldspar prepared by ion-exchange of microcline (McMillan et al. 1980). The cell parameters of rubicline determined from refinement of electron diffraction data are of much lower accuracy and precision compared to the cell parameters determined using conventional X-ray powder diffraction (McMillan et al. 1980) for rubidium feldspar of similar composition (Table 3). Nevertheless, within the accuracy of the method, the TEM cell parameters are reasonably close to those expected for a triclinic rubidium feldspar. The coherency of structure from well-ordered microcline to rubicline also supports an exsolution origin for an (Al,Si)-ordered rubidium feldspar.

TABLE 2. Rubidium feldspar *d*-spacings (Å)

$^*d_{meas}$	$^*d_{calc}$	*h*	*k*	*l*
5.82	5.814	0	$\bar{1}$	1
5.77	5.775	0	1	1
4.62	4.607	0	2	1
3.88	3.855	1	3	0
3.61	3.616	$\bar{0}$	3	1
3.60	3.596	$\bar{1}$	$\bar{3}$	1
3.59	3.588	$\bar{0}$	$\bar{3}$	1
2.94	2.938	$\bar{1}$	$\bar{4}$	1
2.65	2.653	$\bar{2}$	$\bar{2}$	1
2.63	2.633	$\bar{2}$	$\bar{4}$	1
2.61	2.607	$\bar{3}$	1	0
2.56	2.562	$\bar{2}$	4	1

* *d*-values were measured from indexed electron-diffraction patterns. The differences between d_{meas} and d_{calc} are quite large, reflecting the intrinsically lower accuracy and precision of electron diffraction relative to conventional diffractometry.

ORIGIN OF RUBICLINE

Rubicline, ideally $RbAlSi_3O_8$, is the first mineral to contain essential rubidium and is a new member of the feldspar group, forming a solid-solution series with microcline. It occurs in pollucite-bearing rare-element granitic pegmatites that attain a high degree of alkali-metal fractionation. The primary potassium feldspar was probably (Al,Si)-disordered and monoclinic, and had considerably higher concentrations of Na, Rb, and P than currently occur in the host microcline. In K-rich feldspar, the monoclinic → triclinic transition results from (Al,Si)-ordering rather than framework collapse, and precedes exsolution of albite (Brown and Parsons 1989). Textural features suggest that rubicline exsolution postdated that of albite, probably due to the slower rate of diffusion of Rb compared to that of Na (Giletti 1994).

The microcline-rubicline exsolution does not texturally resemble the lamellar form typical of solid-state reactions. The most probable reason for the irregular shape of rubicline, and its diffuse transition into the K-dominant host, is the very small dimensional and angular difference between the unit cells of end-member microcline and rubicline (e.g., McMillan et al. 1980). The differences are, of course, still smaller between intermediate members of the (K-Rb) series that constitute most of the exsolved

TABLE 3. Comparison of cell dimensions for synthetic rubicline ($Rb_{0.56}K_{0.44}$) and rubicline ($Rb_{0.57}K_{0.41}Cs_{0.02}$)

	Synthetic*	Natural†
a (Å)	8.758(3)	8.81(3)
b	12.967(3)	13.01(3)
c	7.243(3)	7.18(4)
α (°)	90.56(1)	90.3(1)
β	116.08(2)	115.7(3)
γ	87.93(1)	88.2(1)

* McMillan et al. (1980).
† This work. The cell parameters agree within 2 standard deviations.

pairs of feldspars. The exsolution amounts to small-scale migration of alkalis in an aluminosilcate framework that suffers only very minor distortion and preserves perfect three-dimensional coherence between the exsolved phases. It is, however, conceivable that the present-day textures reflect a degree of fluid-induced modification, which may also be suggested by the silica-excess composition of some of the rubicline and by its local association with quartz.

The processes of (Al,Si)-ordering and exsolution are catalyzed by H_2O; however, a $\square Si_4O_8$ substitution, which may allow partial occupancy of the feldspar M-site by H_2O, has been recently identified and shown to be widespread in potassium feldspar from the hydrous environment of granitic pegmatites (Teertstra et al. 1998a). At Elba, substitution of $\square Si_4O_8$ in microcline does not exceed the "detection limit" of 1 mol%; however, up to 4 mol% $\square Si_4O_8$ occurs in rubicline. The primary feldspar may have been hydrous and contained more Si than is now present in microcline. Typically, the $\square Si_4O_8$ component occurs in all generations of feldspar at a given locality, or is absent from all of them. The Elba feldspars do not follow this pattern; quartz may have exsolved during the structural microcline-forming phase transition. Rubicline may have formed by diffusion of Rb^+ and nucleation in the $\square Si_4O_8$-rich microcline surrounding grains of quartz. The occurrence of rubicline surrounding grains of quartz is also unique to this locality.

Acknowledgments

We thank W.L. Brown and H. Kroll for their comments on this manuscript. This work was supported by NSERC Operating, Major Installation, Equipment, and Infrastructure Grants to P.Č. and F.C.H. D.K.T. was supported by a University of Manitoba Duff Roblin Fellowship. The TEM work was done in the Electron Microbeam Analysis Facility in the Department of Earth and Planetary Sciences, University of New Mexico. We thank Ecole des Mines, Paris, for donation of pollucite and feldspar specimens.

References cited

Breithaupt, J.F.A. (1846) X. Neue Mineralien. 4 and 5. Kastor und Pollux. Poggendorffs Annalen, 99, 1391–1400.

Brown, W.L. and Parsons, I. (1989) Alkali feldspars: Ordering rates, phase transformations and behaviour digrams for igneous rocks. Mineralogical Magazine, 53, 25–42.

Giletti, B.J. (1994) Isotopic equilibrium/disequilibrium and diffusion kinetics in feldspars. In I. Parsons, Ed., Feldspars and Their Reactions, p. 351–382. NATO ASI Series C, Mathematical and Physical Sciences, Reidel, Boston.

McMillan, P.F., Brown, W.L., and Openshaw, R.E. (1980) The unit-cell parameters of an ordered K-Rb alkali feldspar series. American Mineralogist, 65, 458–464.

Orlandi, P. and Scortecci, P.B. (1985) Minerals of the Elba pegmatites. Mineralogical Record, 16, 353–363.

Pezzotta, F., Hawthorne, F.C., Cooper, M.A., and Teertstra, D.K. (1996) Fibrous foitite from San Piero in Campo, Elba, Italy. Canadian Mineralogist, 34, 741–744.

Pouchou, J.L. and Pichoir, F. (1985) PAP (phi-rho-Z) procedure for improved quantitative microanalysis. In J.T. Armstrong Ed., Microbeam Analysis, p. 104–106. San Francisco Press, California.

Teertstra, D.K., Lahti, S.I., Alviola, R., and Černý, P. (1993) Pollucite and its alteration in Finnish pegmatites. Geological Survey of Finland, Bulletin 368, 1–39.

Teertstra, D.K., Černý, P., and Hawthorne, F.C. (1997) Rubidium-rich feldspars in a granitic pegmatite from the Kola Peninsula, Russia. Canadian Mineralogist, 35, 1277–1281.

Teertstra, D.K., Černý, P., and Hawthorne, F.C. (1998a) Rubidium feldspars in granitic pegmatites. Canadian Mineralogist, in press.

Teertstra, D.K., Hawthorne, F.C., and Černý, P. (1998b) Identification of normal and anomalous composition of minerals by electron-microprobe analysis: K-rich feldspar as a case study. Canadian Mineralogist, 36, 87–96.

Manuscript received December 6, 1997
Manuscript accepted June 22, 1998
Paper handled by Nancy L. Ross